LETTER

doi:10.1038/nature13924

H_2D^+ observations give an age of at least one million years for a cloud core forming Sun-like stars

Sandra Brünken[1], Olli Sipilä[2,3], Edward T. Chambers[1], Jorma Harju[2], Paola Caselli[3,4], Oskar Asvany[1], Cornelia E. Honingh[1], Tomasz Kamiński[5], Karl M. Menten[5], Jürgen Stutzki[1] & Stephan Schlemmer[1]

The age of dense interstellar cloud cores, where stars and planets form, is a crucial parameter in star formation and difficult to measure. Some models predict rapid collapse[1,2], whereas others predict timescales of more than one million years (ref. 3). One possible approach to determining the age is through chemical changes as cloud contraction occurs, in particular through indirect measurements of the ratio of the two spin isomers (ortho/para) of molecular hydrogen, H_2, which decreases monotonically with age[4–6]. This has been done for the dense cloud core L183, for which the deuterium fractionation of diazenylium (N_2H^+) was used as a chemical clock to infer[7] that the core has contracted rapidly (on a timescale of less than 700,000 years). Among astronomically observable molecules, the spin isomers of the deuterated trihydrogen cation, ortho-H_2D^+ and para-H_2D^+, have the most direct chemical connections to H_2 (refs 8–12) and their abundance ratio provides a chemical clock that is sensitive to greater cloud core ages. So far this ratio has not been determined because para-H_2D^+ is very difficult to observe. The detection of its rotational ground-state line has only now become possible thanks to accurate measurements of its transition frequency in the laboratory[13], and recent progress in instrumentation technology[14,15]. Here we report observations of ortho- and para-H_2D^+ emission and absorption, respectively, from the dense cloud core hosting IRAS 16293-2422 A/B, a group of nascent solar-type stars (with ages of less than 100,000 years). Using the ortho/para ratio in conjunction with chemical models, we find that the dense core has been chemically processed for at least one million years. The apparent discrepancy with the earlier N_2H^+ work[7] arises because that chemical clock turns off sooner than the H_2D^+ clock, but both results imply that star-forming dense cores have ages of about one million years, rather than 100,000 years.

We detected the ground-state rotational transition of the para spin isomer of the deuterated trihydrogen cation (para-H_2D^+) at 1.370085 THz (ref. 13) (wavelength $\lambda = 219$ μm) towards IRAS 16293-2422 A/B using the German REceiver for Astronomy at Terahertz frequencies (GREAT[14]) onboard the Stratospheric Observatory For Infrared Astronomy (SOFIA[15]). This line has so far only been tentatively detected in absorption against the bright high-mass star-forming region Orion Irc2 by the Kuiper Airborne Observatory[16]. We also observed the ground-state line of ortho-H_2D^+ at 372.421 GHz (ref. 17) ($\lambda = 0.8$ mm) towards the same source using the Atacama Pathfinder EXperiment (APEX)[18] submillimetre telescope located in the Chilean Atacama desert at an altitude of 5,100 m. IRAS 16293-2422 A/B consists of a triple system of young (<100,000 years) solar-type protostars, comprising a close protobinary (A1/A2) and a third protostar (B) about 600 astronomical units (AU) away from these[19,20], surrounded by a massive envelope (a dense core of about two solar masses) with steeply decreasing (from the inside outward) temperature and density distributions[21,22]. This dense core still bears the physical characteristics typical of starless cores on the verge of star formation (the so-called pre-stellar cores[23]), with the bulk of the material still at low temperatures ($T < 20$ K) and densities (number density of H_2 molecules $n(H_2) < 10^6$ cm^{-3}). The dense core is embedded in the dark cloud Lynds 1689N in Ophiuchus at a distance of 120 pc (ref. 24).

The present observations provide the measurement of the ortho/para H_2D^+ ratio, and thus the corresponding ortho/para H_2 ratio across the dense core (see Methods). The para-H_2D^+ spectrum observed with SOFIA and the ortho-H_2D^+ spectrum observed with APEX are shown in Fig. 1, together with the model predictions (detailed below). We note that para-H_2D^+ shows a strong and narrow absorption profile against the far-infrared continuum emission caused by the central protostellar heating of the surrounding dust grains, while ortho-H_2D^+ is observed in emission with a similar width. These observational facts are related to the cold temperatures of the environment, where almost all para-H_2D^+ is in its rotational ground state (0_{00}) and is therefore observed in absorption (see the energy level diagram in Fig. 1). Owing to the nuclear spin conversion discussed in the Methods, the ground (1_{11}) and the first excited rotational state (1_{10}) of ortho-H_2D^+ are populated even at the low temperature of the dense core. As a consequence, in combination with the lower continuum brightness at larger wavelengths, the major contribution to the ortho-H_2D^+ signal observed at 372 GHz is due to emission (see the energy level diagram in Fig. 1). In what follows, we estimate the amounts of para-H_2D^+ and ortho-H_2D^+ in the line of sight causing the observed absorption and emission features by radiative transfer modelling. It turns out that the ortho/para ratio of H_2D^+ is below 0.1 in the cool outer part of the dense core where the lines originate. This implies a very low ortho/para H_2 ratio in this region.

We model the observed lines using the previously derived dense core structure[22] in conjunction with chemistry and radiative transfer calculations[11,25,26] (see Methods). The radial density distribution of the dense core is described by a power law between the central cavity (radial distance 30 AU from the centre) and the outer edge of the core (6,100 AU). The gas temperature increases strongly inwards in this model owing to gas compression in the collapse and to radiation from the protostars. In agreement with several previous studies of this region[27], we assume that the dense core is embedded in an ambient cloud with typical dark cloud conditions ($n(H_2) \approx 10^4$ cm^{-3}, $T \approx 10$ K; see Extended Data Fig. 1). According to our modelling results, most of the para-H_2D^+ absorption (83%) and nearly all ortho-H_2D^+ emission (91%) originate in the dense core at radial distances from the centre between 2,000 AU and 6,100 AU, where the kinetic temperature decreases from ~20 K to ~13 K, and the hydrogen density $n(H_2)$ decreases from about 10^6 cm^{-3} to about 10^5 cm^{-3} (see Extended Data Fig. 1). This region still preserves the conditions of the original pre-stellar core. The para- and ortho-H_2D^+ spectra produced by our best-fit model are displayed in Fig. 1, together with the observed spectra. The best-fit model predicts an average ortho/para H_2D^+ ratio of 0.07 ± 0.03 between 2,000 AU and 6,100 AU.

Such a low value for the ortho/para H_2D^+ ratio can only be understood as a temporal decrease in parallel with a decreasing ortho/para H_2 ratio. The time evolution of the chemical abundances in different parts of the dense core and in the ambient cloud was calculated using

[1]I. Physikalisches Institut, Universität zu Köln, Zülpicher Straße 77, 50937 Köln, Germany. [2]Department of Physics, PO Box 64, 00014 University of Helsinki, Finland. [3]Max-Planck Institut für Extraterrestrische Physik, Gießenbachstraße 1, 85741 Garching bei München, Germany. [4]School of Physics and Astronomy, University of Leeds, Leeds LS2 9JT, UK. [5]Max-Planck Institut für Radioastronomie, Auf dem Hügel 69, 53121 Bonn, Germany.

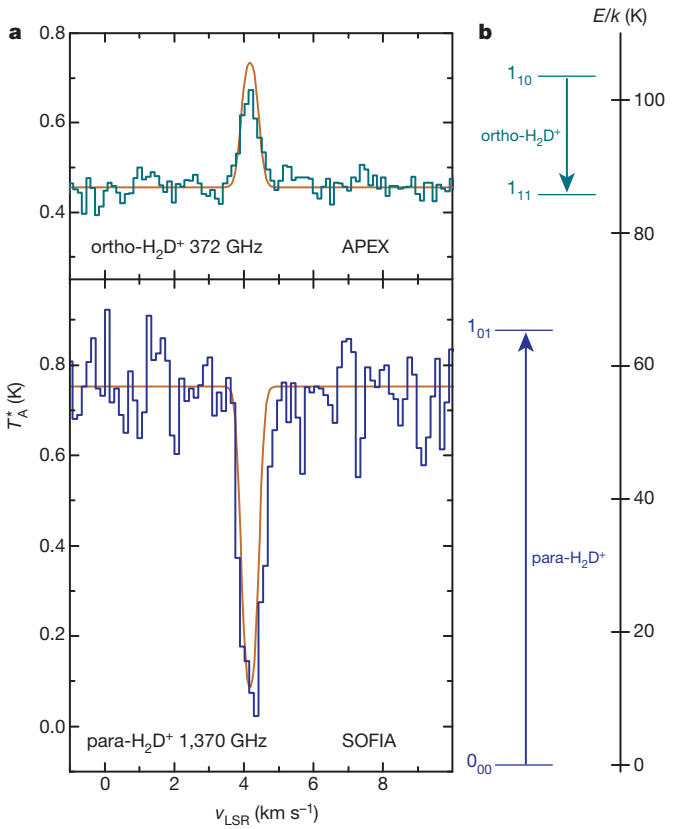

Figure 1 | Observed and modelled H_2D^+ spectra. **a**, The histograms show the ortho-H_2D^+ (top) and para-H_2D^+ (bottom) rotational ground-state lines as observed with APEX/FLASH and SOFIA/GREAT, respectively; the orange lines show the modelled line profiles. Intensities are given as antenna temperatures T_A^* and v_{LSR} denotes the velocity with respect to the local standard of rest. **b**, Energy level diagram (in units of temperature, E/k, where k is the Boltzmann constant) of the lowest rotational states of ortho- and para-H_2D^+.

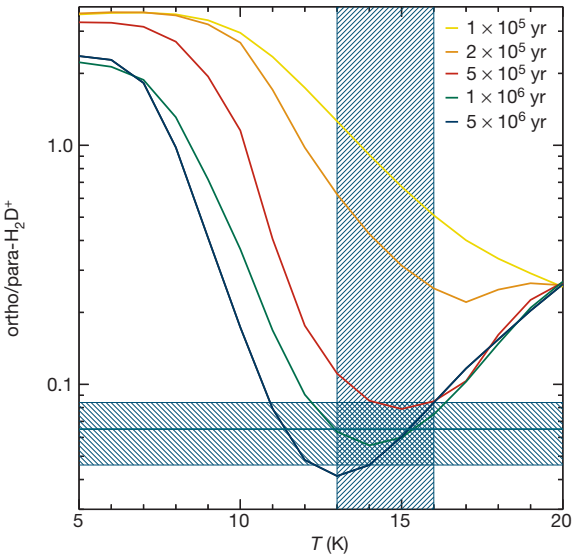

Figure 2 | Modelled ortho/para H_2D^+ abundance ratio. At kinetic temperatures T above ~12 K, the ortho/para H_2D^+ ratio is completely determined in reactions with ortho- and para-H_2, and it is closely tied to the evolution of the ortho/para H_2 ratio. The shaded vertical region indicates the temperature range applicable to the dense core surrounding IRAS 16293-2422 A/B (at radial distances from the core centre of 3,000–6100 AU), while the horizontal shade indicates the observed ortho/para H_2D^+ ratio. Together, these limits suggest a dense core age of at least one million years. The gas density, $n(H_2) = 10^5\ cm^{-3}$, and the visual extinction, $A_V = 10$ mag, are kept constant in this model.

our gas-grain chemistry model[25]. The resulting radial abundance distributions of para- and ortho-H_2D^+, together with the density, temperature and velocity profiles, were used as input for a Monte Carlo radiative transfer program[26] designed to predict observable line profiles. The excitation of the rotational transitions of H_2D^+ in collisions with para- and ortho-H_2 are calculated using theoretical state-to-state rate coefficients[11]. The slow conversion of ortho- to para-H_2, together with the coupling of the ortho/para H_2 ratio to that of H_3^+ and its deuterated species through proton exchange reactions (see Extended Data Fig. 2) allows us to use the observed ortho/para H_2D^+ ratio as a chemical clock for the dense core age since the time of its formation within the ambient cloud.

Using conservative values of the initial ortho/para H_2 ratio in our time-dependent chemical models (see Methods), the low values of the ortho/para H_2D^+ ratio (~0.065 ± 0.019) found in the outermost layers of the dense core with $T = 13$–16 K can only be reached after about a million years of chemical evolution, preceded by a period at least equally long in conditions corresponding to the embedding ambient dark cloud. To illustrate the temporal evolution of the ortho/para H_2D^+ ratio in conditions corresponding to the dense core surrounding IRAS 16293-2422 A/B, we plot this ratio in Fig. 2 as a function of the kinetic temperature of the environment for different evolution times after the formation of the dense core. Owing to the restrictions in dense core temperature and the observed ortho/para H_2D^+ ratio (shown as vertical and horizontal shaded areas, respectively, in Fig. 2), the temporal evolution of the dense core is at least one million years (see Methods).

Therefore, we have verified that the observed ortho/para H_2D^+ ratio is setting limits on the core age. The ortho/para H_2D^+ ratio gives a more direct estimate of the ortho/para H_2 ratio than the previously used deuterium fraction measurement of N_2H^+ (that is, N_2D^+/N_2H^+; ref. 7), in particular for evolved regions with ortho/para H_2 ratios of less than 0.01. Below this value, the N_2D^+/N_2H^+ ratio loses correlation with the ortho/para H_2 ratio (see Extended Data Figs 3 and 4). Therefore, at this point, the N_2D^+/N_2H^+ chemical clock stops while the clock based on the ortho/para H_2D^+ ratio keeps running. Our results indicate that the average ortho/para H_2 ratio is about 2×10^{-4} between radii of 3,000 AU and 6,100 AU ($T = 13$–16 K), which can be reproduced only at very late times of chemical evolution (see Extended Data Fig. 5). Our conservative analysis gives an age estimate of at least one million years. The very low value of ortho/para H_2 found in the core around IRAS16293-2422 is hardly possible to probe by any other means, and we conclude that the timing set by the ortho/para H_2D^+ ratio is most relevant for constraining the duration of the dense cloud core phase in the course of star formation.

Online Content Methods, along with any additional Extended Data display items and Source Data, are available in the online version of the paper; references unique to these sections appear only in the online paper.

Received 7 July; accepted 6 October 2014.
Published online 17 November 2014.

1. Ward-Thompson, D. *et al.* An observational perspective of low-mass dense cores. II: Evolution toward the initial mass function. In *Protostars and Planets* **V** (eds Reipurth, B., Jewitt, A. P. & Keil, K.) 33–46 (Univ. Arizona Press, 2007).
2. Hartmann, L., Ballesteros-Paredes, J. & Heitsch, F. Rapid star formation and global gravitational collapse. *Mon. Not. R. Astron. Soc.* **420,** 1457–1461 (2012).
3. Mouschovias, T. Ch., Tassis, K. & Kunz, M. W. Observational constraints on the ages of molecular clouds and the star formation timescale: ambipolar-diffusion-controlled or turbulence-induced star formation? *Astrophys. J.* **646,** 1043 (2006).
4. Flower, D. R. & Watt, G. D. On the ortho-H_2/para-H_2 ratio in molecular clouds. *Mon. Not. R. Astron. Soc.* **209,** 25–31 (1984).
5. Flower, D. R., Pineau Des Forêts, G. & Walmsley, C. M. The importance of the ortho:para H_2 ratio for the deuteration of molecules during pre-protostellar collapse. *Astron. Astrophys.* **449,** 621–629 (2006).
6. Pagani, L., Roueff, E. & Lesaffre, P. Ortho-H_2 and the age of interstellar dark clouds. *Astrophys. J.* **739,** L35 (2011).

7. Pagani, L. *et al.* Ortho-H_2 and the age of prestellar cores. *Astron. Astrophys.* **551,** A38 (2013).
8. Pagani, L., Salez, M. & Wennier, P. G. The chemistry of H_2D^+ in cold clouds. *Astron. Astrophys.* **258,** 479–488 (1992).
9. Gerlich, D., Herbst, E. & Roueff, E. $H_3^+ + HD \rightarrow H_2D^+ + H_2$: low-temperature laboratory measurements and interstellar implications. *Planet. Space Sci.* **50,** 1275–1285 (2002).
10. Hugo, E., Asvany, O., Harju, J. & Schlemmer, S. Toward understanding of H_3^+ isotopic and nuclear spin fractionations in cold space. In *Molecules in Space and Laboratory* (eds Lemaire, J. L. & Combes, F.) 119 (S. Diana, 2007).
11. Hugo, E., Asvany, O. & Schlemmer, S. $H_3^+ + H_2$ isotopic system at low temperatures: microcanonical model and experimental study. *J. Chem. Phys.* **130,** 164302 (2009).
12. Sipilä, O. *et al.* Modelling line emision of deuterated H_3^+ from prestellar cores. *Astron. Astrophys.* **509,** A98 (2010).
13. Asvany, O. *et al.* High-resolution rotational spectroscopy in a cold ion trap: H_2D^+ and D_2H^+. *Phys. Rev. Lett.* **100,** 233004 (2008).
14. Heyminck, S. *et al.* GREAT: the SOFIA high-frequency heterodyne instrument. *Astron. Astrophys.* **542,** L1 (2012).
15. Young, E. T. *et al.* Early science with SOFIA, the Stratospheric Observatory For Infrared Astronomy. *Astrophys. J.* **749,** L17 (2012).
16. Boreiko, R. T. & Betz, A. L. A search for the rotational transitions of H_2D^+ at 1370 GHz and H_3O^+ at 985 GHz. *Astrophys. J.* **405,** L39–L42 (1993).
17. Amano, T. & Hirao, T. Accurate rest frequencies of submillimeter-wave lines of H_2D^+ and D_2H^+. *J. Mol. Spec.* **233,** 7 (2005).
18. Güsten, R. *et al.* The Atacama Pathfinder EXperiment (APEX)—a new submillimeter facility for southern skies. *Astron. Astrophys.* **454,** L13 (2006).
19. Wootten, A. The duplicity of IRAS 16293–2422: a protobinary star? *Astrophys. J.* **337,** 858–864 (1989).
20. Girart, J. M., Estalella, R., Palau, A., Torrelles, J. M. & Rao, R. On the origin of the molecular outflows in IRAS 16293–2422. *Astrophys. J.* **780,** L11 (2014).
21. Stark, R. *et al.* Probing the early stages of low-mass star formation in LDN 1689N: dust and water in IRAS 16293–2422A, B, and E. *Astrophys. J.* **608,** 341–364 (2004).
22. Crimier, N. *et al.* The solar type protostar IRAS16293–2422: new constraints on the physical structure. *Astron. Astrophys.* **519,** A65 (2010).
23. Keto, E. & Caselli, P. Dynamics and depletion in thermally supercritical starless cores. *Mon. Not. R. Astron. Soc.* **402,** 1625 (2010).
24. Lombardi, M., Lada, C. J. & Alves, J. Hipparcos distance estimates of the Ophiuchus and the Lupus cloud complexes. *Astron. Astrophys.* **480,** 785–792 (2008).
25. Sipilä, O., Caselli, P. & Harju, J. HD depletion in starless cores. *Astron. Astrophys.* **554,** A92 (2013).
26. Juvela, M. Non-LTE radiative transfer in clumpy molecular clouds. *Astron. Astrophys.* **322,** 943–961 (1997).
27. Le Gal, R. *et al.* Interstellar chemistry of nitrogen hydrides in dark clouds. *Astron. Astrophys.* **562,** A83 (2014).

Acknowledgements GREAT is a development by the MPI für Radioastronomie and the KOSMA/Universität zu Köln, in cooperation with the MPI für Sonnensystemforschung and the DLR Institut für Planetenforschung. SOFIA is jointly operated by the Universities Space Research Association, Inc. (USRA), under NASA contract NAS2-97001, and the Deutsches SOFIA Institut (DSI) under DLR contract 50 OK 0901 to the University of Stuttgart. APEX, the Atacama Pathfinder Experiment, is a collaboration between the Max Planck Institut für Radioastronomie (MPIfR), the Onsala Space Observatory (OSO), and the European Southern Observatory (ESO). This work has been supported by the Collaborative Research Centre 956, funded by the Deutsche Forschungsgemeinschaft (DFG). O.S. and J.H. acknowledge support from the Academy of Finland grants 132291 and 250741. P.C. acknowledges the financial support of the European Research Council (ERC; project PALs 320620).

Author Contributions S.S., S.B., O.A., P.C., J.H., O.S. and J.S. jointly designed the study and proposed the SOFIA observations. E.T.C. performed the calibration and the analysis of the SOFIA data. C.E.H. was instrumental in developing the GREAT receiver. T.K. and K.M.M. made the APEX observations and analysed these data. O.S. carried out the chemistry and radiative transfer modelling with help from J.H. The paper was jointly written by S.B., J.H., O.S., P.C. and S.S. All authors discussed the results and commented on the manuscript.

Author Information Reprints and permissions information is available at www.nature.com/reprints. The authors declare no competing financial interests. Readers are welcome to comment on the online version of the paper. Correspondence and requests for materials should be addressed to S.B. (bruenken@ph1.uni-koeln.de) or S.S. (schlemmer@ph1.uni-koeln.de).

METHODS

Observational strategy. Although the rotational ground-state emission line of ortho-H_2D^+ has been observed towards several cold starless and low-mass star-forming cores[21,28], para-H_2D^+ has previously been detected only tentatively, in absorption towards the Orion IRc2 region using the NASA Kuiper Airborne Observatory (KAO)[16]. The ground-state rotational transition of para-H_2D^+ at 1.37 THz is extremely difficult to observe from the ground owing to poor atmospheric transmission and the resulting large system temperatures at terahertz frequencies. The transition frequency was not covered by the Herschel/HIFI bands[29]. The GREAT[14] receiver onboard SOFIA[15] now enables us to observe para-H_2D^+. Despite its rather high upper-state energy (66 K above ground) the para-H_2D^+ line at 1.37 THz can be excited in cold, dense cores. However, the expected brightness temperature of the emission line is very weak. Absorption against a bright continuum source is the best way of detecting the line with currently available instruments in a reasonable observing time. Because H_2D^+ is most abundant in cold gas deficient in CO[30], the best chance of detecting the para-H_2D^+ line is by observing it towards a young (Class 0)[31] protostar with bright continuum emission surrounded by a massive, cool envelope. IRAS 16293-2422 A/B is one of the best targets fulfilling these criteria.

SOFIA observations. We observed the para-H_2D^+ ground-state transition $J_{KaKc} = 0_{00}–1_{01}$ at 1370.085 GHz ($\lambda = 219$ μm)[13] towards IRAS 16293-2422 A/B using the GREAT instrument[14] onboard SOFIA[15] on 23 July 2013 during SOFIA's southern deployment to New Zealand in Cycle 1 operations. The target position was: right ascension 16 h 32 m 22.9 s, declination −24° 28′ 39″ (J2000). We used the GREAT L1a channel (1.25–1.40 THz) with the XFFTS backend[32], which has a bandwidth of 2.5 GHz and a channel spacing of 88 kHz (17 ms^{-1}). We operated the instrument in the double beam-switch mode, with a chopping frequency of 1 Hz, a chop amplitude of 20″ (for a total beam throw of 40″), and a chop angle of 0° from horizontal in the telescope reference frame. In total, we had an on-source integration time of ~26 min (system temperature $T_{sys} = 1{,}760$ K). We calibrated the data using the standard pipeline (*kalibrate*[33]), which fits an atmospheric model to the observed sky to calculate the atmospheric opacity. The forward and main beam efficiencies for the L1 channel on GREAT are 0.97 and 0.67, respectively. The half-power beam width (HPBW) of the 2.5-m SOFIA telescope is ~22″ at 1,370 GHz.

During observations we noticed a slow drop-off of the continuum level as the telescope drifted away from the nominal source position, caused by the lack of good tracking stars in the heavily extinct region around IRAS 16293-2422 A/B. We had to re-acquire the source three times. Because the continuum level is of vital importance for this absorption measurement, we averaged our data in such a way that the nominal continuum value of the source was conserved. To determine this continuum level, we averaged the continuum level calculated in each of the spectra obtained after reacquisition (four chop-nod pairs) using a large number of line-free channels. The nominal continuum intensity, measured on the equivalent antenna temperature scale, of $T^*_{A,C} = 0.79 \pm 0.03$ K, obtained in this way agrees very well with the flux density of 460 Jy that we obtained from an analysis of archival Herschel/SPIRE (Spectral and Photometric Imaging Receiver) and PACS (Photoconductor Array Camera and Spectrometer) continuum maps. This nominal value was then used to re-scale all of the other averaged pairs. We calculated the weighted average of the remaining spectra using a $1/\sigma^2_{rms}$ weighting, so that the spectra with the weakest original continuum (the highest root-mean-square (r.m.s.) noise after re-scaling) have the smallest contribution to the final spectrum. Finally, to correct for the double-sideband reception of GREAT, we subtracted half of the continuum from the spectrum (assuming equal gains in the two sidebands). A Gaussian fit to the para-H_2D^+ absorption spectrum smoothed to a velocity resolution of 0.13 km s^{-1} gives the following line parameters: velocity with respect to the local standard of rest $v_{LSR} = 4.24 \pm 0.02$ km s^{-1}, line width (in units of velocity) $\Delta v = 0.73 \pm 0.05$ km s^{-1}, and $T^*_A - T^*_{A,C} = -0.70 \pm 0.07$ K (the difference between the 219-μm continuum and the antenna temperature at the line centre). The observed para-H_2D^+ spectrum is compatible with total absorption in the line centre, which implies a very large optical depth and a low excitation temperature for the para-H_2D^+ line.

APEX observations. The target position as indicated above was observed in the $J_{KaKc} = 1_{10}–1_{11}$ ortho ground-state transition of H_2D^+ at 372.421 GHz ($\lambda = 805$ μm)[17] using the 12-m APEX telescope[18] on 5 and 14 August 2013 in excellent weather conditions. We used the lower-frequency module (covering 262–374 GHz) of the upgraded version of the First Light APEX Submillimetre Heterodyne instrument (FLASH[34]). FLASH is a two-sideband receiver with a bandwidth of 4 GHz for each sideband. On the two observing days we used different frequency settings that covered the sky frequency of the ortho-H_2D^+ line. We employed the 4-GHz total bandwidth (per intermediate frequency) of the newest version of the APEX facility Fast Fourier Transform Spectrometer (FFTS[35]). The FFTS band was split into 104,859 channels with a spacing of 38.2 kHz, which corresponds to 31 m s^{-1} at 372.4 GHz. The calibration was achieved by the standard chopper-wheel method. The background was subtracted by means of wobbling sub-reflector, using a beam throw of 150″ and a switching rate of 0.7 Hz. In total we spent ~50 min on source ($T_{sys} = 590$ K). Conversion of the measured antenna temperatures to flux density units (in Jy) and a main-beam brightness temperature, T_{MB}, scale (in K) was established by interpolating previously determined aperture and main-beam efficiencies[18], η_A and η_{MB}, which yielded $\eta_A = 0.58$ and $\eta_{MB} = 0.68$. The HPBW of the antenna is 17″ at 372 GHz. Fitting a Gaussian to our pointing drift scans yields a deconvolved source size of 12″ (FWHM). The baseline level in the spectra gave a flux density of 18.6 ± 1.7 Jy for the continuum source (antenna temperature at APEX $T^*_{A,C} = 0.47 \pm 0.04$ K). These values are in good agreement with previous measurements[21]. We estimate a 20% error for our intensity calibration from the difference of the two spectra summed up for each observing date. This is larger than typical FLASH calibration errors, but explainable by the fact that the line frequency lies in the wings of deep atmospheric O_2 and H_2O absorption lines (at 368 GHz and 380 GHz, respectively). A Gaussian fit to the ortho-H_2D^+ spectrum smoothed to a velocity resolution of 0.12 km s^{-1} gives the following line parameters: $v_{LSR} = 4.17 \pm 0.02$ km^{-1}, $\Delta v = 0.62 \pm 0.05$ km^{-1}, and $T^*_A - T^*_{A,C} = 0.21 \pm 0.02$ K, consistent with the velocity position and width of the para-H_2D^+ line at 1.37 THz.

Both our peak and our integrated main-beam brightness temperatures are a factor of ~3 lower than the published values measured with the 15-m James Clerk Maxwell Telescope (JCMT)[21]. These previous measurements were probably positioned within a few arcseconds of our pointing. The large difference is not explainable by the slightly different antenna sizes. We found archival H_2D^+ spectra towards our target source taken with the HARP instrument on the JCMT on three different dates, 7 and 8 August 2007, and 21 February 2008. The summed spectrum, while noisy, agrees with ours within the uncertainties.

Source model. The dense core surrounding IRAS 16293-2422 A/B is known to have steep density and temperature gradients. Therefore, the standard method for deriving column densities from observed spectra based on the assumption of line-of-sight homogeneity is not likely to give reliable results. We adopt a frequently used physical model for IRAS 16293-2422 A/B (ref. 22), where the radial density distribution of the dense core is described by a power law, $n(H_2) \propto r^{-1.8}$, between the central cavity (30 AU) and the outer edge (6,100 AU, corresponding to 51″ at a distance of 120 pc), see Extended Data Fig. 1. The gas temperature increases strongly inwards in this model because of gas compression in the collapse and due to the radiation from the protostars. Infall speeds are significant in warm inner parts of the dense core where the abundance of H_2D^+ is negligible. Recent observations with Herschel/HIFI[27,36] imply the presence of a low-density absorbing layer in front of the dense core, which can probably be attributed to the ambient dark cloud Lynds 1689. We therefore add to the dense core a spherically symmetric, ambient cloud ($n(H_2) = 10^4$ cm^{-3}, $T = 10$ K) with a thickness causing a visual extinction of $A_V = 10$ mag to the outer edge of the dense cloud. Our radiative transfer calculations show that this ambient cloud deepens slightly the para-H_2D^+ absorption, and causes self-absorption to the ortho-H_2D^+ emission. For the purposes of chemistry modelling and radiative transfer calculations, the model is divided into concentric shells where the density and temperature are assumed to be constant.

The ortho/para H_2 ratio. Molecular hydrogen is formed when two hydrogen atoms react on dust grains. The spins of the two protons ($I = 1/2$) in H_2 give rise to four nuclear spin states, three with total nuclear spin $I = 1$ (ortho-H_2) and degenerate spin orientations ($m_I = -1, 0, 1$), and one with total nuclear spin $I = 0$ (para-H_2) and no degeneracy ($m_I = 0$). Each of those states is formed with equal probability, implying a statistical ortho/para ratio of H_2, of 3:1. As a result of the Pauli exclusion principle, ortho nuclear spin states are connected to the energy states with odd rotational quantum numbers J, while para spin states are found at rotational levels with even J. As a consequence, the odd (ortho) and even (para) rotational state populations of H_2 are far from thermodynamical equilibrium upon formation, especially in cold molecular clouds. After entering the gas phase, the ortho/para-H_2 ratio is altered by proton-exchange reactions, whereas conversion between ortho- and para-H_2 by radiation and inelastic collisions is spin-forbidden. The dominant spin-changing reactions are those with H^+ and H_3^+. These well-studied reactions[9,11,37,38] can thermalize ortho/para-H_2 efficiently in warm gas, whereas below 20 K, ortho/para-H_2 approaches thermal equilibrium very slowly as proton exchange reactions have to compete with the more favoured ortho production on grains. At the typical dark cloud kinetic temperature, $T = 10$ K, the thermal ortho/para-H_2 is as low as 3.6×10^{-7}. However, this value is probably never reached. According to chemistry models[5,25,39], ortho/para-H_2 remains suprathermal in very cold gas (<12 K). It is the subtle detail of the indistinguishable two fermions (protons) in H_2, in combination with the spin changing proton exchange reactions, that turn ortho/para-H_2 into a robust chemical clock in cold molecular clouds[4,5,39] (see also Extended Data Fig. 5).

Analytical relation between the H_2 and H_2D^+ ortho/para ratios. The ortho/para ratio of H_2D^+ in molecular clouds is mainly regulated by the following chemical reactions[9,10]:

$$\text{para-}H_2D^+ + \text{ortho-}H_2 \Leftrightarrow \text{ortho-}H_2D^+ + \text{para-}H_2 \quad (1)$$

$$\text{ortho-}H_2D^+ + \text{ortho-}H_2 \Leftrightarrow \text{para-}H_2D^+ + \text{para-}H_2 \quad (2)$$

$$\text{ortho-}H_2D^+ + \text{ortho-}H_2 \Leftrightarrow \text{para-}H_2D^+ + \text{ortho-}H_2 \quad (3)$$

The reaction ortho-H_2D^+ + ortho-H_2 → ortho/para-H_3^+ + HD, returning deuterium back to deuterated hydrogen (HD), occurs about three times more slowly than the ortho-to-para conversion described by reactions (2) and (3) (ref. 11). Also, the further conversion of H_2D^+ to D_2H^+ is slower than the ortho-to-para conversion because ortho-H_2 is always more abundant than HD. From the reaction system described above, the following analytic expression can be derived for the equilibrium ortho/para-H_2D^+ (ref. 10):

$$\frac{[\text{ortho–}H_2D^+]}{[\text{para–}H_2D^+]} = \frac{(k_1^+ + k_3^-) \times [\text{ortho–}H_2]/[\text{para–}H_2] + k_2^-}{(k_2^+ + k_3^+) \times [\text{ortho–}H_2]/[\text{para–}H_2] + k_1^-}$$

where k_1^+, k_1^-, k_2^+, k_2^-, k_3^+ and k_3^- are the rate coefficients of the forward (+) and backward (−) direction of reactions (1), (2) and (3). As shown below, this simple relation, using the Arrhenius behaviour of the rate coefficients[9,10], approximates the ortho/para-H_2D^+ predicted by comprehensive chemical models. This emphasizes the direct correlation between the ortho/para ratios of H_2D^+ and H_2 that is the central tool of this work.

Chemistry model. The time-evolution of the chemical abundances in different parts of the dense core surrounding IRAS 16293-2422 A/B and in the embedding ambient cloud is calculated using a chemistry model containing reaction sets for both gas-phase and grain surface chemistry[25]. The gas-phase reaction set is based on the publicly available Ohio State University reaction set (available upon request from Eric Herbst, eh2ef@virginia.edu), which has been expanded to include the spin states of the light hydrogen-bearing species H_2^+, H_2, and H_3^+. In addition, deuterated species with up to four atoms and their reaction rates are included. Similar ortho/para separation and deuteration as in the gas phase is applied to the surface reaction set, which is based on a previously published model[40]. The model is pseudo-time-dependent, that is, we follow the chemical evolution assuming that the dense core and the ambient cloud are static. We assume that the initial chemical composition of the dense core is determined in conditions corresponding to the ambient cloud ($n(H_2) = 10^4$ cm^{-3}). Therefore, we calculate molecular abundances at different times in the ambient cloud and use these abundances as initial conditions for the dense core model. In the ambient cloud, the gas is assumed to be initially atomic, with the exception of hydrogen, which is molecular. We have fixed the cosmic-ray ionization rate to $\zeta = 1.3 \times 10^{-17}$ s^{-1}, the grain radius to $a_g = 0.1$ μm, and the initial ortho/para-H_2 to 1.0×10^{-3}, corresponding to a spin temperature of $T_{spin} \approx$ 20 K. This assumption is based on the fact that the ortho/para ratio is possibly thermalized by collisions with protons (H^+) in warm gas down to ~20 K during the contraction and cooling phase of the cloud. Efficient thermalization down to ~30 K has been demonstrated previously[5,39,41]. Starting the simulation from an initial ortho/para-H_2 of 0.5 ($T_{spin} \approx 60$ K), which is typical for diffuse interstellar clouds[42], it takes about 3–4 million years of chemical processing in conditions corresponding to the ambient cloud to reduce ortho/para-H_2 to ~10^{-3}. By comparison with the observed ortho- and para-H_2D^+ lines, we obtain the same chemical age of about a million years for the dense core (see below) using either the high and the low initial ortho/para-H_2 ratio, although in the former case the ambient cloud has to be very old (more than 3 million years).

The ortho/para-H_2D^+ ratio, as a function of ortho/para-H_2, resulting from the full simulation closely follows the analytical formula presented above[10]. This is illustrated in Extended Data Fig. 2, which shows the relationship for different kinetic temperatures and for ortho/para-$H_2 < 0.1$, roughly corresponding to times after 100,000 years of chemical evolution. The fact that reactions (1) to (3) dominate the relative abundances of ortho-H_2D^+ and para-H_2D^+ in this regime can also be verified by inspecting the actual reaction rates during the simulation. At low values of ortho/para-H_2 for which $(k_2^+ + k_3^+) \times$ ortho/para-$H_2 \ll k_1^-$, ortho/para-H_2D^+ is linearly proportional to ortho/para-H_2. For high values of ortho/para-H_2 for which $(k_2^+ + k_3^+) \times$ ortho/para-$H_2 \gg k_1^-$, ortho/para-H_2D^+ approaches a constant, which, according to the analytical formula, is determined by the ratio $(k_1^+ + k_3^-)/(k_2^+ + k_3^+)$. The full simulation predicts a slightly lower asymptotic value of ortho/para-H_2D^+, which can be attributed mainly to the reaction ortho-H_2D^+ + ortho-H_2 → ortho/para-H_3^+ + HD.

The disagreement between the analytical formula and the simulation is most marked at very low temperatures (<10 K), where the deuteration reactions H_3^+ + HD → H_2D^+ + H_2 and H_2D^+ + HD → D_2H^+ + H_2 influence ortho/para-H_2D^+. The importance of these reactions depends on the H_3^+ abundance, which is sensitive to the cosmic-ray ionization rate ζ and the grain radius a_g. When $T > 10$ K, the relationship between ortho/para-H_2D^+ and ortho/para-H_2 is almost independent of other physical conditions than the kinetic temperature. The ortho/para-H_2 ratio has been previously derived by modelling the deuterium fraction of the HCO^+ and N_2H^+ molecular ions[6,7,39]. This is based on the fact that the DCO^+/HCO^+ and N_2D^+/N_2H^+ abundance ratios show a general increasing trend with a decreasing ortho/para-H_2. As shown in Extended Data Figs 3 and 4, the relationships N_2D^+/N_2H^+ and DCO^+/HCO^+ (not plotted) versus ortho/para-H_2 also depend (besides on T) on $n(H_2)$, ζ, and a_g. The ortho/para-H_2D^+ versus ortho/para-H_2 relationship for the same parameter space is shown for comparison. It is evident that in conditions where ortho/para-$H_2 < 0.01$ (corresponding roughly to $N_2D^+/N_2H^+ > 0.01$), ortho/para-H_2D^+ gives a better estimate for ortho/para-H_2 than N_2D^+/N_2H^+. We note, however, that the accuracy of the N_2D^+/N_2H^+ method can be substantially improved by mapping observations of the N_2D^+ and N_2H^+ distributions[7]. At even longer evolutionary times N_2D^+/N_2H^+ actually becomes independent of ortho/para-H_2, whereas ortho/para-H_2D^+ can still be used as a chemical clock. This is the regime of ortho/para-H_2 that is relevant in studies of old pre-stellar cores.

Radiative transfer calculations. The resulting radial abundance distributions of para-H_2D^+ and ortho-H_2D^+, together with the density, temperature and velocity profiles, were used as input for a Monte Carlo radiative transfer program[26] to predict the line profiles observed with the telescopes used in the present study. The excitation of the rotational transitions of H_2D^+ in collisions with para- and ortho-H_2 are calculated using theoretically determined state-to-state rate coefficients[11]. We calculate the radial distributions of the optical thicknesses and the excitation temperatures of the ground-state transitions of para- and ortho-H_2D^+ as a function of velocity, and construct the observable absorption/emission spectra, taking into account the continuum source in the centre of the dense core, and the beam profile of the respective telescopes. We ran multiple models corresponding to different ages of the initial cloud and of the dense core itself. Six different time steps between 10,000 years and 2 million years were considered. We searched for the best match between the modelled and observed line profiles by performing a χ^2 test for each model, simultaneously for the two lines. From this analysis, we find that the model with a million years of chemical evolution in both the initial cloud stage and in the dense core yields the best fit to the observations. In this case the optical thickness in the line centre is determined to be $\tau_o = 0.33$ for the ortho-H_2D^+ line and to be $\tau_p = 2.7$ for the para-H_2D^+ line. The fractional abundance relative to H_2 of both ortho- and para-H_2D^+ increases with the distance from the source centre, reaching 10^{-10} and 10^{-9}, respectively, at the outer edge of the envelope (at a radius of 6,100 AU).

Possibility of detecting para-H_2D^+ in other sources. IRAS 16293-2422 A/B is one of the brightest far-infrared sources in nearby molecular clouds and provides a particularly favourable target for observing para-H_2D^+ in absorption. A quick look at archival Herschel continuum maps of nearby complexes[43], including Chamaeleon, Corona Australis, Ophiuchus, Perseus, Serpens and Taurus, reveals eight embedded Class 0/I protostars or protoclusters with far-infrared flux densities at least 25% of that of IRAS 16293. We estimate that para-H_2D^+ absorption from a dense core similar to that surrounding IRAS 16293 could be detected towards these weaker sources in approximately 1.5 h with SOFIA/GREAT. The Herschel maps, together with Spitzer archival catalogues, can be used to select embedded sources with massive envelopes that are likely to be most appropriate for para-H_2D^+ absorption observations[44].

28. Caselli, P. *et al.* Survey of ortho-H_2D^+ ($1_{1,0}$-$1_{1,1}$) in dense cloud cores. *Astron. Astrophys.* **492,** 703–718 (2008).
29. de Graauw, T. *et al.* The *Herschel*-Heterodyne Instrument for the Far-Infrared (HIFI). *Astron. Astrophys.* **518,** L6 (2010).
30. Caselli, P., van der Tak, F. F. S., Ceccarelli, C. & Bacmann, A. Abundant H_2D^+ in the pre-stellar core L1544. *Astron. Astrophys.* **403,** L37–L41 (2003).
31. André, Ph, Ward-Thompson, D. & Barsony, M. From prestellar cores to protostars: the initial conditions of star formation. In *Protostars and Planets IV* (eds Mannings, V., Boss, A. P. & Russell, S. S.) 59–96 (Univ. Arizona Press, 2000).
32. Klein, B. *et al.* High-resolution wide-band fast Fourier transform spectrometers. *Astron. Astrophys.* **542,** L3 (2012).
33. Guan, X. *et al.* GREAT/SOFIA atmospheric calibration. *Astron. Astrophys.* **542,** L4 (2012).
34. Heyminck, S., Kasemann, C., Güsten, R., de Lange, G. & Graf, U. U. The first-light APEX submillimeter heterodyne instrument FLASH. *Astron. Astrophys.* **454,** L21 (2006).
35. Klein, B. *et al.* The APEX digital Fast Fourier Transform spectrometer. *Astron. Astrophys.* **454,** L29 (2006).
36. Coutens, A. *et al.* Heavy water stratification in a low-mass protostar. *Astron. Astrophys.* **553,** A75 (2013).
37. Grussie, F. *et al.* The low-temperature nuclear spin equilibrium of H_3^+ in collisions with H_2. *Astron. Astrophys.* **759,** 21 (2012).
38. Honvault, P., Jorfi, M., González-Lezana, T., Faure, A. & Pagani, L. Ortho-para H_2 conversion by proton exchange at low temperature: an accurate quantum mechanical study. *Phys. Rev. Lett.* **107,** 023201 (2011); Erratum: *Phys. Rev. Lett.* **108,** 109903 (2012).
39. Pagani, L. *et al.* Chemical modeling of L183/L134N: an estimate of the ortho/para H_2 ratio. *Astron. Astrophys.* **494,** 623–636 (2009).
40. Semenov, D. *et al.* Chemistry in disks. IV. Benchmarking gas-grain chemical models with surface reactions. *Astron. Astrophys.* **522,** A42 (2010).

41. Albertsson, T. *et al.* First time-dependent study of H_2 and H_3^+ ortho-para chemistry in the diffuse ISM. *Astrophys. J.* **787,** 44 (2014).
42. Crabtree, K. N., Indriolo, N., Kreckel, H., Tom, B. A. & McCall, B. J. On the ortho:para ratio of H_3^+ in diffuse molecular clouds. *Astrophys. J.* **729,** 15 (2011).
43. André, P. *et al.* From filamentary clouds to prestellar cores to the stellar IMF: initial highlights from the Herschel Gould Belt Survey. *Astron. Astrophys.* **518,** L102 (2010).
44. Sadavoy, S. I. *et al.* Class 0 protostars in the Perseus molecular cloud: a correlation between the youngest protostars and the dense gas distribution. *Astrophys. J.* **787,** L18 (2014).

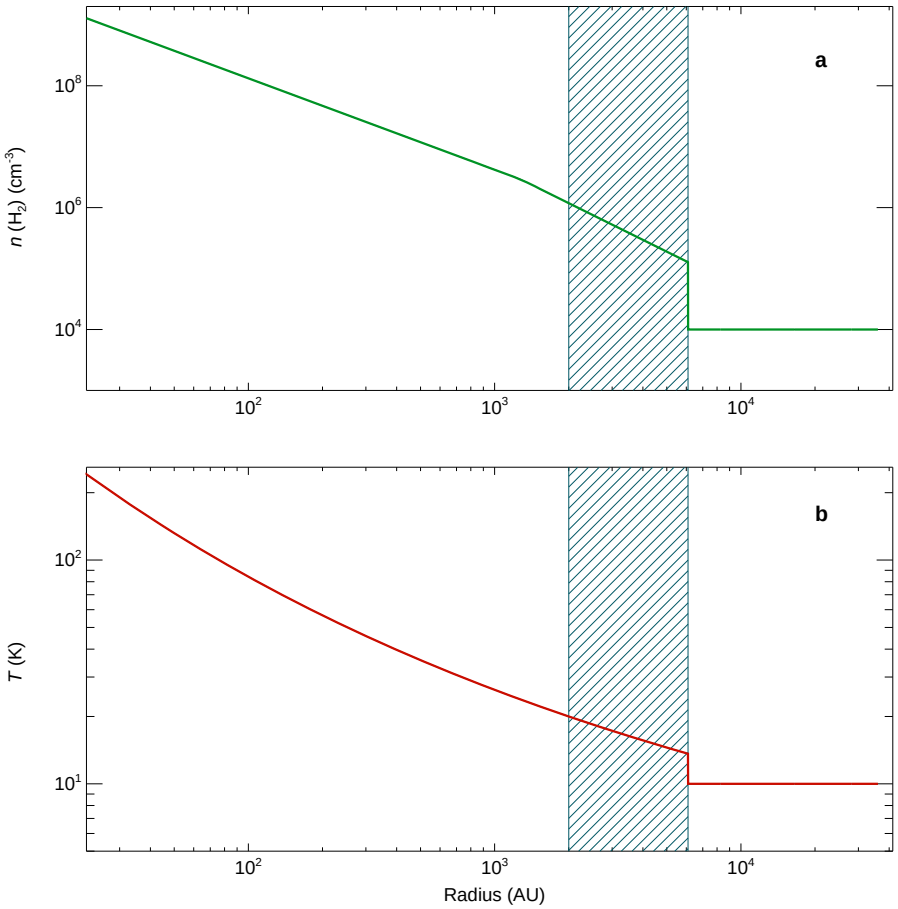

Extended Data Figure 1 | Temperature and density distribution of the source model. Physical model of IRAS 16293-2422 A/B, consisting of a widely used core model[22] and a low-density ambient cloud. **a**, The number density $n(H_2)$ as a function of radius. **b**, The radial profile of the kinetic temperature, T. The ambient cloud is assumed to have $n(H_2) = 10^4\,cm^{-3}$ and $T = 10\,K$. The shaded interval, between a radius of 3,000 and 6,100 AU, represents the outer envelope of the core, which dominates the observed para-H_2D^+ absorption and ortho-H_2D^+ emission.

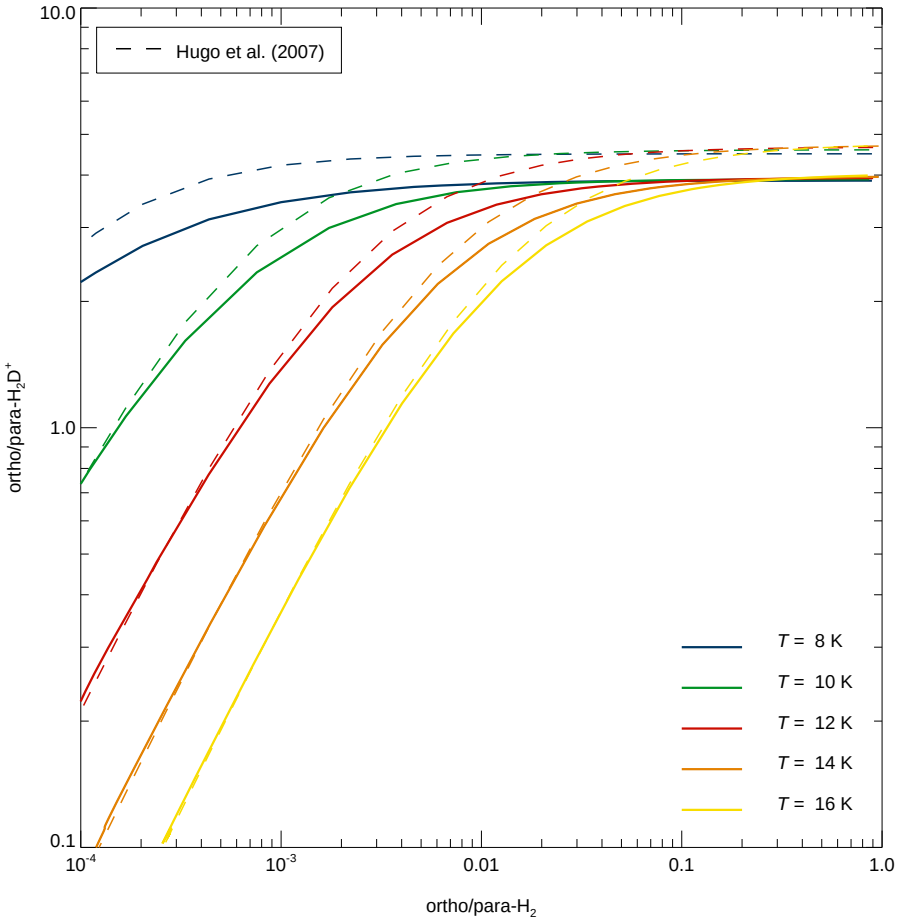

Extended Data Figure 2 | The relationship between ortho/para-H_2D^+ and ortho/para-H_2. The ortho/para-H_2D^+ ratio as a function of ortho/para-H_2 resulting from chemistry simulations for different values of the kinetic temperature T, indicated with colours. The dashed curves represent the approximation given by the analytical formula from Hugo *et al.*[10].

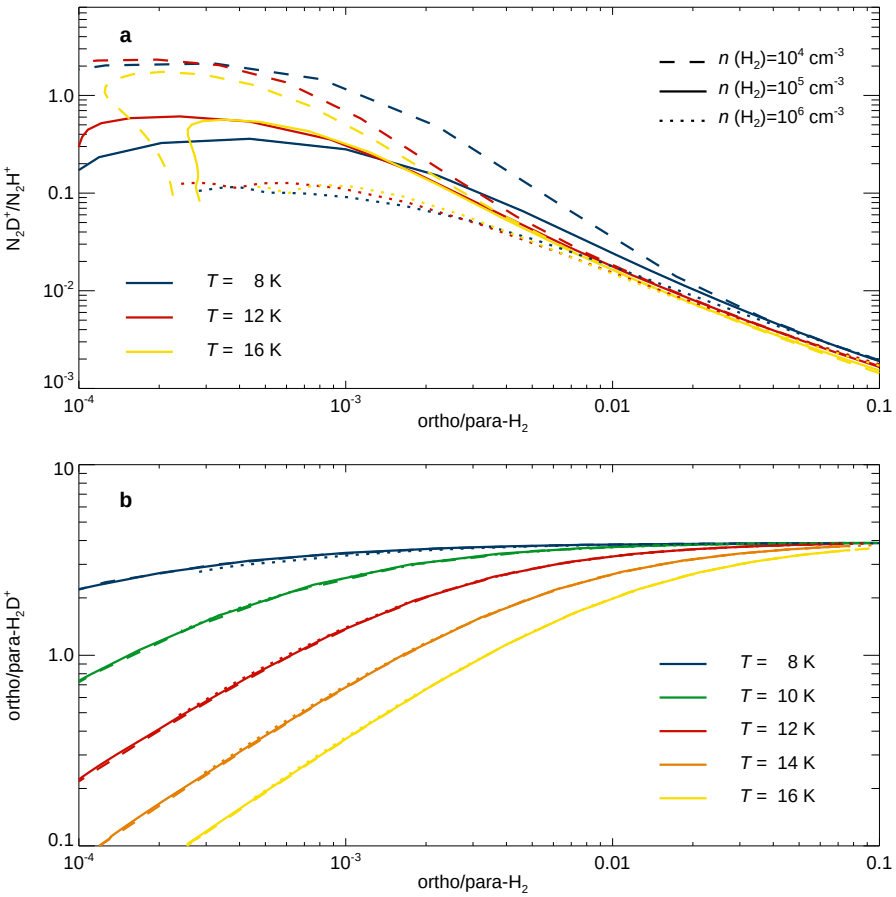

Extended Data Figure 3 | N_2D^+/N_2H^+ and ortho/para-H_2D^+ as functions of ortho/para-H_2, for different values of T and $n(H_2)$. **a**, The N_2D^+/N_2H^+ abundance ratio versus the ortho/para H_2 ratio for selected values of the kinetic temperature, T, and the H_2 number density, $n(H_2)$. **b**: The ortho/para H_2D^+ ratio versus the ortho/para H_2 ratio for different temperatures and densities. One can see that this relationship depends on T but not on $n(H_2)$.

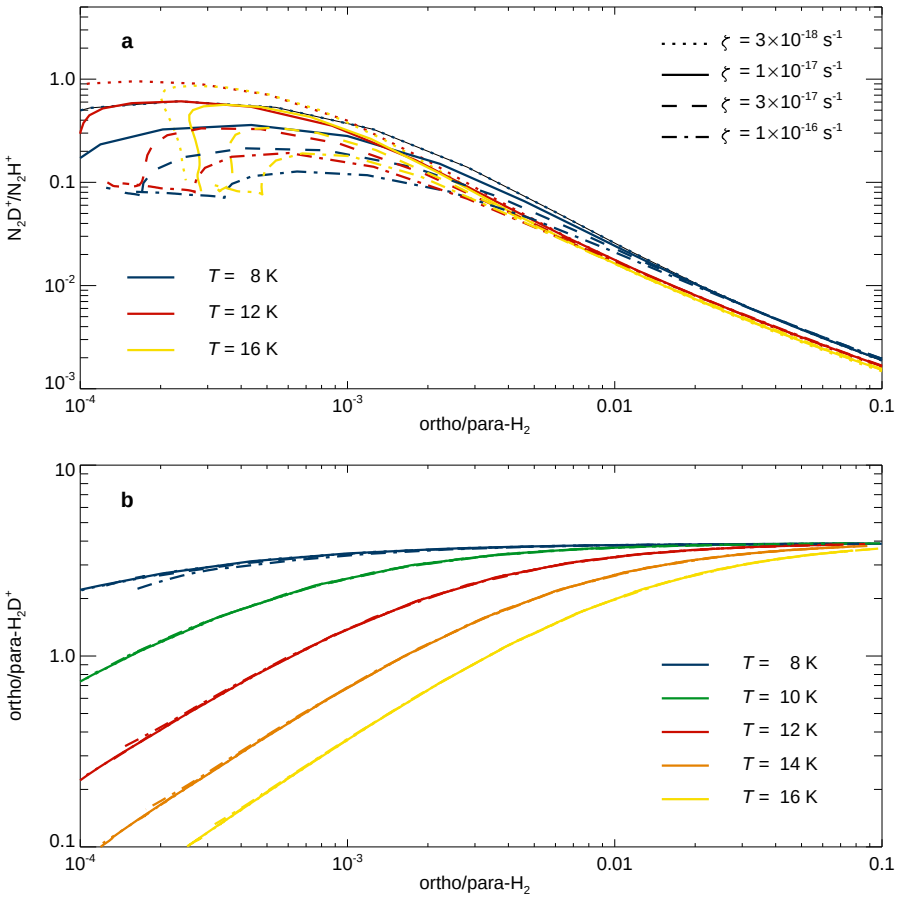

Extended Data Figure 4 | N_2D^+/N_2H^+ and ortho/para-H_2D^+ as functions of ortho/para-H_2, for different values of T and ζ. **a**, The N_2D^+/N_2H^+ abundance ratio versus the ortho/para H_2 ratio for selected values of the kinetic temperature, T, and the cosmic ray ionization rate, ζ. **b**, The same for the ortho/para H_2D^+ ratio versus the ortho/para H_2 ratio for different temperatures and densities $n(H_2)$. Hardly any dependence on ζ is seen except at the lowest temperatures.

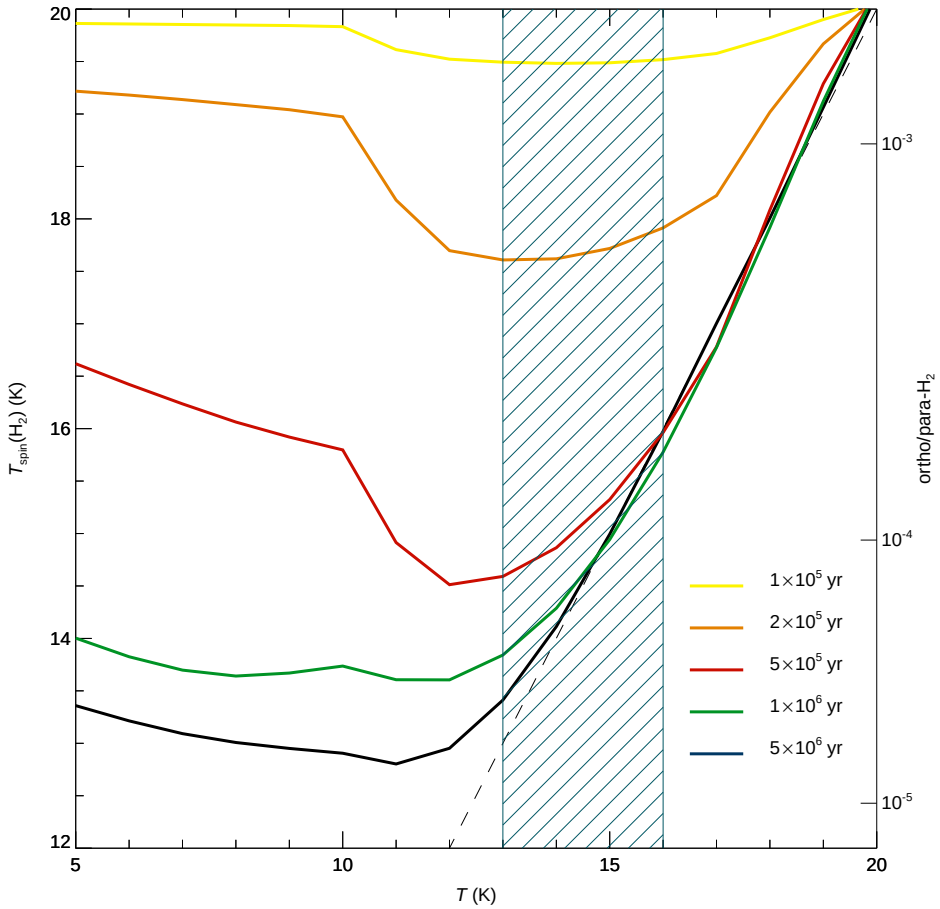

Extended Data Figure 5 | The H_2 spin temperature. Variation of the H_2 spin temperature T_{spin} as a function of kinetic temperature and time in a dark cloud according to our gas-grain chemistry model. The corresponding ortho/para-H_2 is indicated on the right. The gas density, $n(H_2) = 10^5\,cm^{-3}$, and the visual extinction, $A_V = 10$ mag, are kept constant. Ortho/para-H_2 tends for long evolutionary times towards the thermal values (dashed line) above $T_{kin} \approx 12$ K. The blue-hatched region indicates the T range applicable to the dense core surrounding IRAS 16293-2422 A/B (between a radius of 3,000 and 6,100 AU).